

Attention as Annotation: Generating Images and Pseudo-masks for Weakly Supervised Semantic Segmentation with Diffusion

Ryota Yoshihashi, Yuya Otsuka, Kenji Doi, Tomohiro Tanaka

Yahoo Japan Corporation

Abstract

Although recent advancements in diffusion models enabled high-fidelity and diverse image generation, training of discriminative models largely depends on collections of massive real images and their manual annotation. Here, we present a training method for semantic segmentation that neither relies on real images nor manual annotation. The proposed method *attn2mask* utilizes images generated by a text-to-image diffusion model in combination with its internal text-to-image cross-attention as supervisory pseudo-masks. Since the text-to-image generator is trained with image-caption pairs but without pixel-wise labels, *attn2mask* can be regarded as a weakly supervised segmentation method overall. Experiments show that *attn2mask* achieves promising results in PASCAL VOC for not using real training data for segmentation at all, and it is also useful to scale up segmentation to a more-class scenario, i.e., ImageNet segmentation. It also shows adaptation ability with LoRA-based fine-tuning, which enables the transfer to a distant domain i.e., Cityscapes.

Introduction

Generative modeling in images is a task to estimate distributions of natural images and enable the sampling of new images from them. Although the generation of natural-looking images has been a long-standing challenge, recent diffusion models (Ho, Jain, and Abbeel 2020) brought rapid advancement for stable training of high-fidelity image generative models. Particularly, diffusion models trained with large-scale web-crawled image-text pairs (Schuhmann et al. 2021) enabled highly controllable text-to-image synthesis (text2img) (Ramesh et al. 2021; Rombach et al. 2022), which can reflect prompting by free-form texts into the generated contents.

In contrast, the training of image-recognition models largely depends on supervised learning using massive manual annotations on image collections (Deng et al. 2009). An extreme case is semantic segmentation, where we need pixel-wise class labeling in each training image to exploit the full supervision. Weakly supervised learning (WS), a methodology to utilize coarser signals such as boxes or image-level labels (Oquab et al. 2015), has been extensively

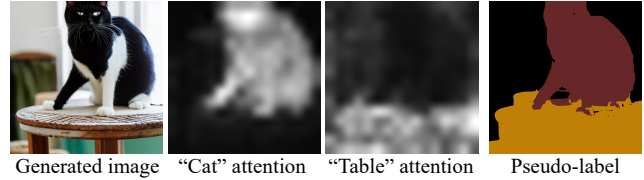


Figure 1: Proposed method *attn2mask* uses generated images paired with pseudo-mask computed from generative attentions per prompt token for semantic segmentation.

studied in segmentation to mitigate this labor. Although recent WS methods have achieved preferable segmentation qualities in the benchmarks (Everingham et al. 2015), complex techniques are often needed to acquire pseudo-masks with satisfactory quality, which limits the generality of the methods. Furthermore, WS can not mitigate the necessity to gather images that are annotatable and aligned to the deployment (or test) domain.

Here, our idea is to leverage the advanced generative models to synthesize images and corresponding pseudo-labels jointly. Generative models’ generation processes may contain semantics of the images generated by themselves, which are reusable for training another recognition model. We propose *attn2mask*, a semantic-segmentation training method that exploits synthesized images and internal attention maps from a text2img diffusion model as supervisory signals, as illustrated in Fig. 1. *Attn2mask* can be regarded as a WS method since it only requires image-text pairs in training the generative model and no pixel-annotated image. However, *attn2mask*’s difference from the existing WS method is that it requires no real images in training its segmentation model, which reduces image collection labor once the text2img model is trained (or downloaded from public model hubs).

While we demonstrate that a simple combination of off-the-shell Stable Diffusion (Rombach et al. 2022) and a supervised segmentation method (Chen et al. 2018) work unexpectedly well, we further investigate approaches for improvements from two viewpoints: 1) robust segmentation training and 2) domain adaptation. The former is based on the observation that the diffusion-based pseudo-masks are sometimes not very accurate due to leaking into back-

grounds or missing parts of objects, and we find that a real-image-based WS training method (Rong et al. 2023) can mitigate harmful effects from this, even in training with synthesized images. For the latter, we develop an unsupervised domain adaptation technique using test-domain images (but not labels) for our image-mask generator, apart from the purely synthesized-based training. This adaptation opens the possibility of exploiting generic image generators in new domains where the generators are not intended.

In experiments, we verify attn2mask’s effectiveness by achieving 58.3 mIoU in the PASCAL VOC segmentation task, which is accurate for not using any real images or annotation. Attn2mask is also applicable to a larger-scale scenario in ImageNet-S 1k-class segmentation, where it performs sufficiently close to the semi-supervised BigDataset-GAN generator. Furthermore, an adaptation of Stable Diffusion using a small amount of target-domain images is shown to be beneficial for distant-domain transfer for the Cityscapes driving images, although it is a bit apart from the spirit of real-image-free training.

Our contributions are summarized as follows: 1) We show that off-the-shelf Stable Diffusion without any modification or fine-tuning can generate images and pseudo-masks that have sufficient quality to train semantic-segmentation models. 2) We improve the synthetic training results by incorporating a robust training method using co-training. 3) We present a domain-adaptive image-and-pseudo-mask generation method with Stable Diffusion exploiting LoRA to make attn2mask applicable to distant-domain tasks.

Related work

Segmentation with diffusion models

Several studies have tried to leverage the diffusion models’ excellent image-generation performance in segmentation. There are two lines of research: reusing diffusion U-Net for segmentation tasks and generating training image-label pairs for segmentation. For the former line, it was shown that denoising diffusion probabilistic models (DDPMs) can be used as pre-trained feature extractors for semantic segmentation (Baranchuk et al. 2022). ODISE (Xu et al. 2023) similarly fine-tunes a text2img diffusion model for segmentation, but it enables phrase-based segmentation by reusing a text encoder in the text2img model. This usage of text2img models as visual-linguistic backbones can be seen as a generative counterpart of contrastive visual-linguistic foundation models, i.g., CLIP (Radford et al. 2021), which also can be repurposed for segmentation tasks (Rao et al. 2022). However, all of the aforementioned methods rely on manually annotated pixel labels for training.

For the latter line, Grounded Diffusion (Li et al. 2023) trains image-and-mask generation models by leveraging a pre-trained Mask R-CNN with pixel labels. We refer to this kind of approaches *semi-supervised* mask generation for their dependency on annotated training images on at least partial classes. DiffuMask (Wu et al. 2023) is closer to ours in the sense of *weakly supervised* mask generation, where masks are automatically acquired via text2img generation training. The main difference between DiffuMask and our

attn2mask is that DiffuMask focuses on single-object generation but attn2mask supports multi-object image generation and is usable for training multi-class segmentation models. Note that these studies (Li et al. 2023; Wu et al. 2023) are contemporary to ours.

Training with generated images

The idea of exploiting free annotations with synthesized images dates back before the large-scale generative models: for example, computer-graphics-based dataset creation using game engines was examined (Richter et al. 2016). More primitively, even segmentation of mathematically drawn contours can help real segmentation as a pretraining task (Kataoka et al. 2022). However, such rendered images tended to have gaps from real ones, which needed supervised retraining or unsupervised adaptation techniques (Hoffman et al. 2018) to utilize them fully to achieve preferable real-environment performances. In contrast, we exploit modern generative models’ high-fidelity generation ability that narrows the gap without any adaptation in at least generic settings such as PASCAL VOC. Prior to the diffusion models, GAN-based image-and-mask generation was also tried (Li et al. 2022a) but they still required manual annotation for partial classes to fine-tune the GANs for mask generation. In addition to segmentation, classification (Sariyildiz et al. 2023) and unsupervised representation learning (Tian et al. 2023) with generated images have been studied, and they report performances gradually approaching to real-dataset-based counterparts, which is motivating for studies in synthetic training including ours.

Weakly supervised semantic segmentation

The mainstream of weakly supervised semantic segmentation (WSSS) approaches exploits image-level class labels. Two-stage training that first trains an image-level classifier and then re-trains another segmentation model using the classifier’s class-activation maps (CAM) (Zhou et al. 2016) as weak labels is the most straightforward but still well-used strategy. Among the two-stage methods, existing studies attempted techniques for better CAM generation (Wang et al. 2020; Jo and Yu 2021; Li et al. 2021; Chen et al. 2022) and robust segmentation training against weak labels (Liu et al. 2022; Li et al. 2022b; Rong et al. 2023). From the viewpoint of WSSS, we replace classifier-based CAMs with generative attentions combined with generated images. In addition, we incorporate the latest robust segmentation-training method (Rong et al. 2023), which we confirm to be beneficial in our training scenario.

Unsupervised segmentation and text-based segmentation

Recently, segmentation studies diverged in various training strategies. For example, unsupervised semantic segmentation does not use any form of supervision in the downstream segmentation training (Yu et al. 2021; Cho et al. 2021). Our attn2mask may be seen as unsupervised in the sense that it is annotation-free in the downstream domains,

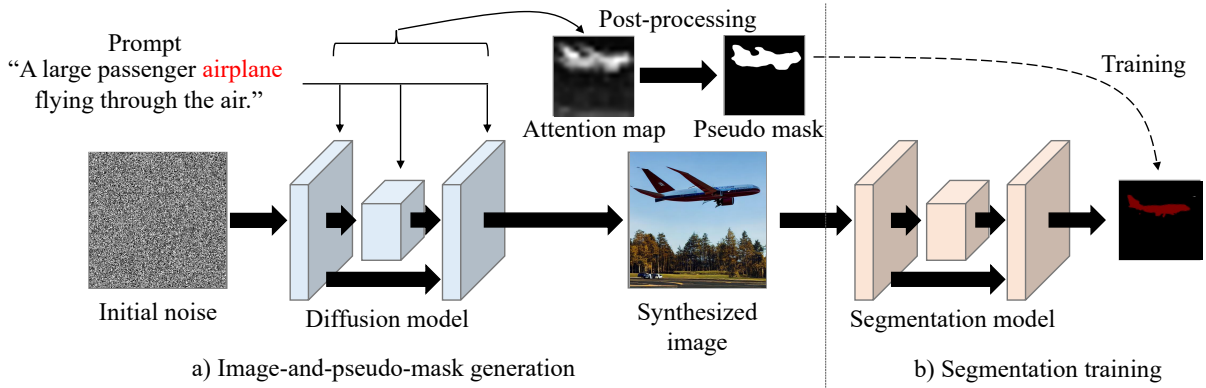


Figure 2: Overview of the proposed method *attn2mask*.

but it operates under the stricter constraint of unavailability of downstream-domain (real) images than usual unsupervised methods. Text-based segmentation exploits large-scale vision-language pretraining (Rao et al. 2022; Zhou, Loy, and Dai 2022; Shin, Xie, and Albanie 2022), which often transfers well in the downstream segmentation tasks without fine-tuning. *Attn2mask* is related to these methods in the usage of vision-language pretraining except for the difference between generative (i.e., Stable Diffusion) and discriminative (i.e., CLIP) pretraining.

Proposed method *Attn2mask*

An overview of *attn2mask* is shown in Fig.2. It consists of a) the image-and-pseudo-mask generation module and b) the segmentation module. We also apply post-processing to the pseudo-masks before passing them to the segmentation model to multi-class binary labels.

Image-and-pseudo-mask generation

To extract semantic regions from diffusion-synthesized images, we need to compute the contributions of each word in the prompts on each location in images. Fortunately, image-text cross-attention, popularly used in most diffusion models including Stable Diffusion, is naturally available for this purpose. Transformer-style attention modules can be written as follows:

$$\text{Transformer}(Q, K, V) = A(Q, K)V, \quad (1)$$

$$A(Q, K) = \text{Softmax}\left(\frac{QK^T}{\sqrt{\dim(K)}}\right), \quad (2)$$

where Q , K , and V are the query, key, and value, each of which is a sequence of vectors, respectively. In using this as text-to-image cross-attention, Q is computed from the image embedding $\mathbf{f} \in \mathbb{R}^{W \times H \times C}$ whose size is $W \times H$ and dimensionality is C , and K and V are computed from the text embedding $\mathbf{s} \in \mathbb{R}^{L \times D}$ whose length is L and dimensionality is D . This makes the attention maps' dimensionality

$$A(Q(\mathbf{s}), K(\mathbf{f})) \in \mathbb{R}^{W \times H \times L}, \quad (3)$$

where the element at (x, y, t) can be interpreted as the amount of contribution from the t -th text token to the location in image coordinate (x, y) .

From the attention maps A , we extract channels that are relevant to the classes of interest to use them as supervisory masks. Given a token sequence of the input prompt, we denote the positions of the relevant tokens of class c by $\tau_c = [t_{c1}, t_{c2}, \dots, t_{cn_c}]$, allowing multiple occurrences of the relevant tokens for a single class. The ‘‘relevance’’ of words and classes is set manually by rule-based matching, for example, listing synonyms for a class’s display name.

$$A_c = \frac{1}{n_c} \sum_{t \in \tau_c} A(Q(\mathbf{s}), K(\mathbf{f}))_t \in \mathbb{R}^{W \times H}, \quad (4)$$

Here, we denote the operation to extract t -th channels of the attention map by $A(\cdot, \cdot)_t$.

We add one more probability map for the background as a class defined by

$$A_0(x, y) = 1.0 - \max_{i \in [1, N]} A_i(x, y) - \beta, \quad (5)$$

which represents the absence of activations for any other classes. Here, β is a hyperparameter to control the strength of the background prior; larger β brings smaller portions of the background area in labeling results. The motivation behind this special treatment for the backgrounds is that they tend to be generated implicitly without concrete indication in the prompts, which makes class-word-based aggregation in Eq. 4 difficult.

After attention maps A_0, A_1, \dots, A_N are gathered, we apply binarization to them to acquire multi-class discrete pseudo-labels. We use the densely connected conditional random field (dCRF) (Krähenbühl and Koltun 2011), a non-learning-based labeling algorithm. This is also useful to improve mask quality by considering the color similarity and local smoothness in labeling. These generation processes are iterated for a given set of prompts, and generated images and masks are stored in the disk as a dataset.

Training segmentation models

Once a dataset of synthesized images and pseudo-labels is generated, any supervised segmentation models are trainable with it in general. However, naive training of supervised learners may suffer since the attention-based pseudo-masks

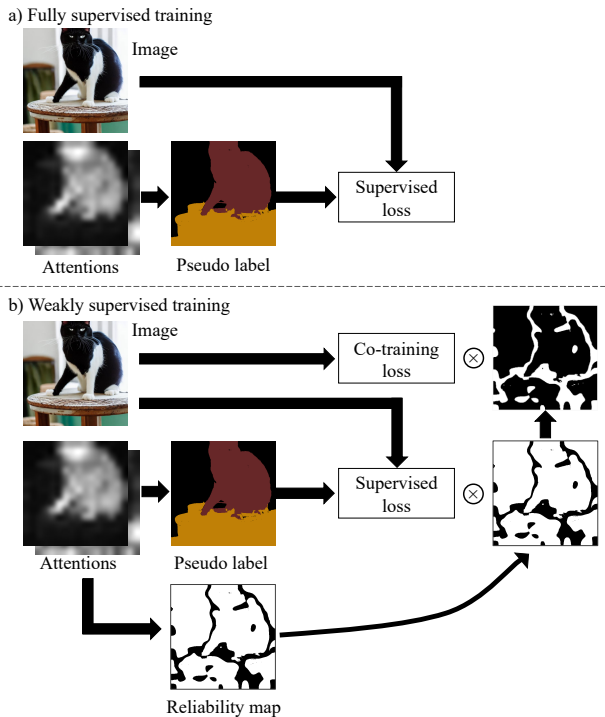


Figure 3: Our fully supervised and weakly supervised training schemes.

are not always perfect in terms of accuracy. Robust learners that are tolerant of label noises would help. Then, we adopt a robust training algorithm from BECO (Rong et al. 2023), a recent WS segmentation method as shown in Fig. 3.

BECO is an adaptive co-training method exploiting reliability maps of the pseudo-labels: It performs supervised learning with full trust in the pseudo-labels within regions where the pseudo-labels are confident and performs co-training-based consistency regularization in regions where the pseudo-labels are unreliable. In the original work, BECO was trained with reliability maps generated by processing the classifier’s confidence score maps. We do not use any classifier and hence simply binarize the attention map to use as the reliability map as follows:

$$R(x, y) = \begin{cases} 1 & \text{if } \max_{i \in [0, N]} A_i(x, y) \geq r \\ 0 & \text{otherwise,} \end{cases} \quad (6)$$

where r is a hyperparameter for the reliability threshold. Other parts in BECO except the reliability map are used unchanged.

Domain adaptive image-mask generation

While image-mask generation with off-the-shelf Stable Diffusion generally performs satisfactorily, in out-of-domain applications, it may suffer from the domain gap between the generative model and the downstream tasks. We notice that this is the case for example, in applying attn2mask to driving images in Cityscapes (Cordts et al. 2016).

To make attn2mask applicable to new domains, we develop an adaptation method using unlabeled training im-

ages. Here, we repurpose the instantiated generation technique DreamBooth (Ruiz et al. 2023) for domain adaptation. For a brief review, DreamBooth learns an instance token (often denoted by [V]) from a relatively small set of instance images. After fine-tuning with the instance-image set, [V] is usable as a new word in prompts to indicate the instance after training. Using DreamBooth, we instead learn a domain token; by training [V] not for a specific instance but for general training images in a new domain, Stable Diffusion can adapt to the domain, while keeping the ability to reflect other prompt words to the image contents.

In implementation, we especially use DreamBooth-LoRA (Hugging Face 2023a), which trains a low-rank adapter (Hu et al. 2022) that is a small sub-network instead of fine-tuning the whole network. This enables fast and stable training with a relatively small target-domain training set.

Experiments

We evaluate semantic-segmentation models trained with attn2mask on three publicly available datasets, namely, PASCAL VOC (Everingham et al. 2015), ImageNet-S (Gao et al. 2022), and Cityscapes (Cordts et al. 2016). We conduct the main experiments in PASCAL VOC, which has been the de facto standard in semantic-segmentation evaluation. While fully supervised learning in VOC seems close to saturation in terms of accuracy, it is challenging enough to tackle without full annotation and real images. Additionally, we evaluate attn2mask’s generalizability to 1) a larger-scale segmentation task with ImageNet-S, which was built on ImageNet-1k (Deng et al. 2009) and 2) a more task-specific scenario with Cityscapes, a dataset toward urban auto-driving.

Dataset generation

We used Stable Diffusion 1.4 (Hugging Face 2023b) trained on LAION-2B (Schuhmann et al. 2021) without modification except in the domain-adaptation settings. We generated 512×512 -resolution images. The attention maps had smaller resolutions but were resized to match the image resolution. Stable Diffusion’s U-Net had multiple cross-attention layers and they were averaged after resizing. We used DDPM (Ho, Jain, and Abbeel 2020) sampler with 100 timesteps, and attention maps were taken at the 50th step. Generation of a sample took around eight seconds with an NVIDIA V100 GPU. Post-processing was conducted using a Python reimplementation of dCRF (Healthcare Intelligence Laboratory 2017) with the default hyperparameters.

The prompt set for VOC was created from the image descriptions from COCO captions (Chen et al. 2015). We curated captions that include VOC class names and their major synonyms that we manually listed up, which made 168,679 captions in total. The prompt set for ImageNet-S was created by a template “a photo of $\{\text{class_name}\}$ with a background”. The variable $\{\text{class_name}\}$ was randomly chosen from the multiple-defined synonyms per class. This made the number of possible varieties of the prompts significantly fewer than the needed samples per class (around 100 images/class) for our experiments, and thus we increased the number of samples by using

Table 1: Segmentation performances on the PASCAL VOC 2012 val set.

Method	bg	aeroplane	bicycle	bird	boat	bottle	bus	car	cat	chair	cow	table
Real-supervised	93.6	88.0	40.0	84.5	66.2	63.2	89.3	84.5	87.6	32.4	74.3	37.6
Attn2mask (ours)	83.0	79.5	33.2	55.7	56.6	56.5	76.3	58.3	70.1	22.2	57.0	34.6
Attn2mask+BECO (ours)	86.6	77.2	29.0	79.0	72.0	56.2	84.8	68.0	80.9	24.9	76.3	46.0

Method	dog	horse	motorbike	person	plant	sheep	sofa	train	tv	mean
Real-supervised	83.0	73.8	78.1	86.1	56.5	76.4	45.0	82.8	71.5	71.2
Attn2mask (ours)	64.7	64.2	55.3	9.0	17.2	57.7	18.7	63.2	38.9	51.1
Attn2mask+BECO (ours)	73.6	71.3	65.9	19.8	22.5	67.8	7.4	68.7	46.1	58.3

Table 2: Comparisons with real-image-based WSSS methods

Method	#Synth. imgs	#Real imgs	mIoU
Attn2mask (ours)	2,000	0	41.2
	10,000	0	46.5
	50,000	0	49.7
	168,679	0	51.1
Attn2mask+BECO (ours)	10,000	0	51.7
	168,679	0	58.3
Pseudo-mask (base)	0	10,582	52.7
ReCAM (base)	0	10,582	54.8
Pseudo-mask (full)	0	10,582	70.0
ReCAM (full)	0	10,582	70.5
BECO (full)	0	10,582	70.9

Table 3: Results in the ImageNet-S FG/BG segmentation evaluated with mIoU.

Method	#Annotations	#Images	
		10k	100k
Real-Supervised	10k	82.1	-
BigDatasetGAN	5k	74.1	74.4
Attn2mask (ours)	0	63.7	66.0

multiple random seeds per prompt. The suffix “with a background” helps to reduce the generation of full-foreground images, which is less useful for training.

For Cityscapes, we used a variable-length template “a photo of $\{\text{class_names}[0]\}$, $\{\text{class_names}[1]\}$, ..., $\{\text{class_names}[n]\}$ in cityscape by a dashboard camera”, where class_names is a random variable-length list of Cityscapes class names. A number of the class names in Cityscapes were not household words that may not be reflected in the generation, and we replaced “terrain” with “sand” and “vegetation” with “plant”. We generated 12k samples. In the adaptation experiments, we used a modified template “a photo of $\{\text{class_names}[0]\}$, $\{\text{class_names}[1]\}$, ..., $\{\text{class_names}[n]\}$ in sks cityscape by a dashboard camera”, where “sks” was the reserved word for the domain token [V] in DreamBooth fine-tuning. More details of this fine-tuning are seen in Appendix.

Table 4: Results in Cityscapes

Method	Adapt.	Acc.	mIoU
Attn2mask (ours)		63.7	13.2
Attn2mask-LoRA (ours)	✓	69.7	17.1
MaskCLIP		35.9	10.0
MDC		-	7.0
PiCIE		-	9.7
ReCo		74.6	19.3
MDC	✓	47.9	7.1
PiCIE	✓	40.7	12.3
STEGO	✓	73.2	21.0
ReCo+	✓	83.7	24.2

Configurations of our model

First, we implemented the simplest version of our proposed method with Stable Diffusion and a fully supervised segmentation model, which we refer to as attn2mask. We used DeepLabv3+ (Chen et al. 2018) with the ResNet50 (He et al. 2016) backbone from the mmsegmentation (MMSegmentation Contributors 2020) codebase. Additionally, we replaced the segmentation training with WS training, which we refer to as attn2mask+BECO; we used the official training codes of BECO (Rong et al. 2023), but it also used DeepLabv3+-ResNet50 and trained models from these two codebases were fully compatible. Reliability threshold r was set to 0.5. Finally, we fine-tuned Stable Diffusion using DreamBooth-LoRA (Hugging Face 2023a) for transfer to Cityscapes, which we refer to as attn2mask-LoRA. We set the base learning rate to 0.01, weight decay to $1e-4$, and total batch size to 32 on 2-GPU machines. We trained real-supervised models for comparisons with the same settings.

Evaluation protocol

For PASCAL VOC and Cityscapes, we followed the official protocol for supervised learners, which is applicable without modification for WS learners including ours. We used the mean intersection-over-union (mIoU) metric. For ImageNet-S, we derived a foreground/background (FG/BG) segmentation task by extracting masks that have the same class labels as their whole images. This was intended to replicate the evaluation protocol of BigDatasetGAN (Li et al. 2022a), in which the authors built their own ImageNet-based segmentation benchmark but it remains unpublished.

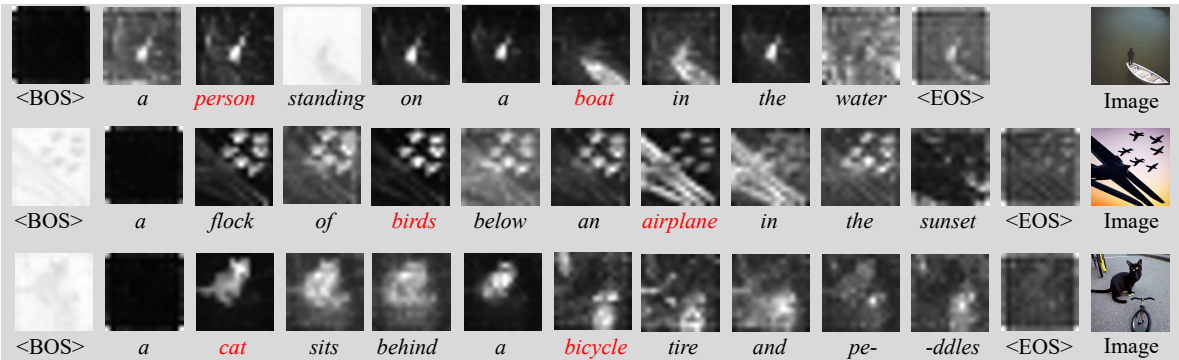


Figure 4: Visualized attention maps corresponding to each of prompt tokens.

Table 5: Variations of post-processing and hyperparameters

Post-processing	mIoU
Thresholding $\theta = 64$	43.5
Thresholding $\theta = 128$	44.6
Otsu	41.2
dCRF $\beta = 0$	44.3
dCRF $\beta = 0.2$	46.5

Table 6: Comparisons with null-text inversion (NTI)

Method	mIoU
Attn2mask	51.1
NTI on the train set and retraining	50.6
NTI on the val set	47.3

Results

Table 1 summarizes the results in VOC. Attn2mask marked mIoU of 51.1%, which is of course worse than the results by supervised training with the real images but surprisingly effective for not using real images or manual annotation at all. In particular, attn2mask performs closely to the supervised counterpart in relatively easy classes such as *aeroplane* (88.0% v.s. 79.5%), *bus* (88.0% v.s. 79.5%), and *horse* (73.8% v.s. 64.2%) or contrarily difficult classes where the supervised models do not work well, such as *bicycle* (40.0% v.s. 33.2%) or *table* (37.6% v.s. 34.6%). We also confirmed that the WS training with BECO benefits our synthetic training, which gained + 7.2%-point improvement on mIoU. However, we also acknowledge that there exists significant degradation of IoU in some classes such as *person*, *plant*, or *sofa* compared with the real-image training. We observed that such classes tend to be generated as parts of backgrounds without being explicitly prompted. This made noise for training these classes, which is the major limitation of our synthetic training.

Table 2 shows comparisons between attn2mask and real-image-based weakly supervised methods. For comparisons, we selected Pseudo-mask matters (Li et al. 2021) and ReCAM (Chen et al. 2022), which were CAM-based and reported baselines that simply learned CAM with their networks. Interestingly, attn2mask with full synthetic images

performed similarly to the baseline weak learners. However, there were gaps between the full configurations of the real-weak learners and attn2mask; the WS training gained +7.2 (51.1 \rightarrow 58.3) mIoU to attn2mask but over 15 points in the real-weak learners (52.7 \rightarrow 70.0 and 54.8 \rightarrow 70.5). These phenomena can be explained by that 1) the domain gaps between real and synthesized images are less dominant when the supervisory signals are weak, and 2) but they become non-negligible as the segmentation models fit tighter with the weakly supervised algorithms.

Table 3 shows the result in ImageNet-S FG/BG segmentation. We compared attn2mask with the same network trained with data from BigDatasetGAN (Li et al. 2022a). BigDatasetGAN is a semi-supervised generator that relies on manual annotation of generated images to fine-tune GAN for mask generation. Attn2mask performed competitively without using pixel-label annotations at all, which is encouraging by showing the ability to freely increase classes within the range Stable Diffusion can generate.

Table 4 shows the results in Cityscapes. In contrast to segmenting object images such as VOC, holistic scene understanding in Cityscapes is extremely challenging for WSSS methods using image-level labels. Hence, unsupervised segmentation methods (Cho et al. 2021; Hamilton et al. 2022; Shin, Xie, and Albanie 2022) are rather intensively developed and we placed reference mIoU values from them. Attn2mask performs similarly to the existing unsupervised methods even with the significant domain gap between web-crawled training images off Stable Diffusion and the driving images. We confirmed the LoRA-based adaptation contributed to the segmentation accuracy, which is encouraging for future development of domain-adaptive diffusion-based segmentation methods. Attn2mask outperformed the strong unsupervised segmentation methods MaskCLIP (Zhou, Loy, and Dai 2022) and PiCIE (Cho et al. 2021) in both settings with and without adaptation. The two methods that outperformed attn2mask relied on test-time heavy computation; STEGO used test-time clustering (Hamilton et al. 2022) and ReCo used retrieval of relevant images for co-segmentation (Shin, Xie, and Albanie 2022).

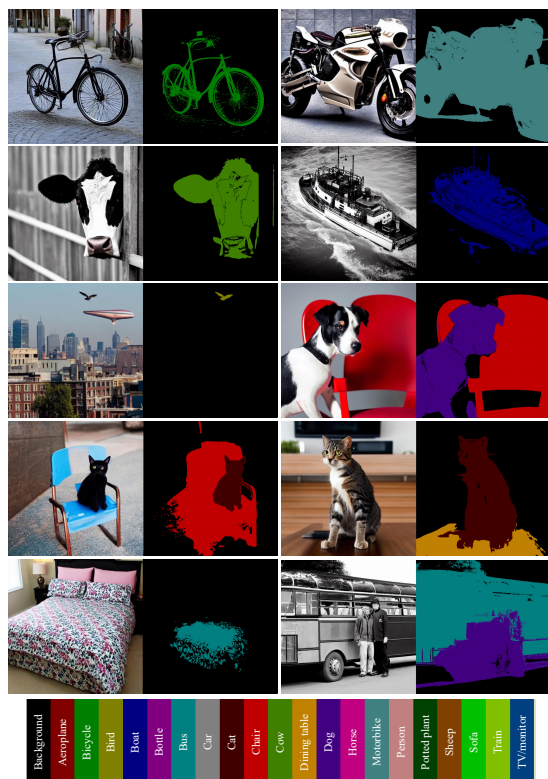


Figure 5: Examples of our training data generated for VOC.

Variations of post-processing

As ablative analyses of post-processing, we tested alternatives of dCRF in the post-processing. Table 5 summarizes the results measured in the attn2mask 10,000-training-data settings. The result shows the effectiveness of dCRF compared with simply applying threshold value θ on the attention maps ranging in $[0, 255]$, or adaptive threshold with Otsu’s method (Otsu 1979).

Stable-Diffusion attention on real images?

We witnessed the surprising effectiveness of Stable Diffusion’s synthesized images and attention maps combined into a segmentation dataset, but raise a new question: *Is this effectiveness solely due to the quality of the attention maps from Stable Diffusion? Do we necessarily need to combine them with synthesized images?* To answer these questions, we attempt to train segmentation models with real images and Stable-Diffusion attentions *projected* on them. For this purpose, we use null-text inversion (Mokady et al. 2022), an inversion method for diffusion models that estimates generation trajectories to generate a given image with a given prompt. The estimated trajectories, i.e., latents at each time-step are used to compute attention maps, and then we can use them as pseudo-labels for segmentation. However, this did not outperform attn2mask despite its additional usage of real images, as shown in Table 6. Using the ground-truth class labels as the prompts, we tried NTI-based pseudo-label generation for VOC training images and direct NTI-based in-

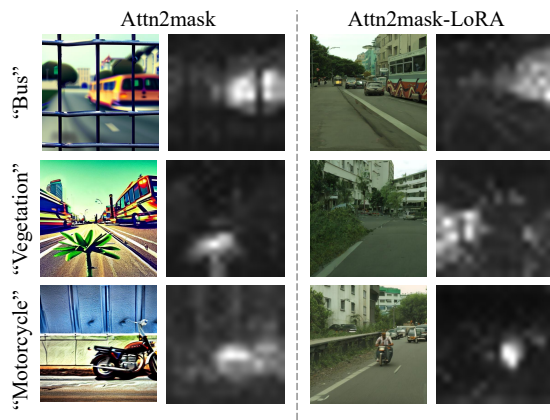


Figure 6: Examples of images and attention maps before and after LoRA-based adaptations in Cityscapes.

ference of the validation images in combination with dCRF post-processing, but both did not outperform attn2mask. This indicates that attentions from Stable Diffusion are particularly good when combined with its own synthesized images, which would support our design of attn2mask.

Visualizations

Figure 4 visualizes examples of the attention maps corresponding to each prompt token. We can see that Stable Diffusion distributes attention well in response to the prompts even in the multi-object generation. This suggests that visual grounding emerges in learning large-scale text2img generation without explicit location-based supervision.

Figure 5 shows examples of generated VOC training images and labels by attn2mask. In addition to the natural-looking object images, it is seen that labels are highly accurate except for several missing detailed parts and overmasking of backgrounds where contextual connections exist, i.g., shadows of objects or waves around boats. We also noticed there exist severe failure cases such as masks not covering whole objects (bottom left) or mismatches of object classes and labels (bottom right).

Figure 6 visualizes synthesized images and attention maps before and after DreamBooth-LoRA-based adaptation. Before adaptation, image contents and styles were not well-aligned with Cityscapes and the naturality of images was also to some extent harmed due to generation in a distant domain from the LAION dataset. After adaptation, generated images look enough like the images in Cityscapes, while attention maps were kept focused on the objects of interest. It is interesting that the correspondence between attention maps and objects is not corrupted after fine-tuning with the Cityscapes images that are not paired with any captions, which might be because DreamBooth-LoRA reuses the prior knowledge acquired in the original Stable Diffusion well.

Conclusion

We presented a real-image-and-annotation-free semantic-segmentation method attn2mask. Although synthetic training did not outperform real-image-based counterparts to the

extent we studied, attn2mask worked surprisingly well for its purely real-image-free segmentation training, and the gaps between the real and synthetic performances were non-negligibly narrow. We hope that this work inspires future studies of generated-image-based methods in more various tasks.

References

- Baranchuk, D.; Voynov, A.; Rubachev, I.; Khrukov, V.; and Babenko, A. 2022. Label-Efficient Semantic Segmentation with Diffusion Models. In *ICLR*.
- Chen, L.-C.; Zhu, Y.; Papandreou, G.; Schroff, F.; and Adam, H. 2018. Encoder-Decoder with Atrous Separable Convolution for Semantic Image Segmentation. In *ECCV*.
- Chen, X.; Fang, H.; Lin, T.-Y.; Vedantam, R.; Gupta, S.; Dollár, P.; and Zitnick, C. L. 2015. Microsoft COCO captions: Data collection and evaluation server. *arXiv preprint arXiv:1504.00325*.
- Chen, Z.; Wang, T.; Wu, X.; Hua, X.-S.; Zhang, H.; and Sun, Q. 2022. Class re-activation maps for weakly-supervised semantic segmentation. In *CVPR*, 969–978.
- Cho, J. H.; Mall, U.; Bala, K.; and Hariharan, B. 2021. PiCIE: Unsupervised semantic segmentation using invariance and equivariance in clustering. In *CVPR*, 16794–16804.
- Cordts, M.; Omran, M.; Ramos, S.; Rehfeld, T.; Enzweiler, M.; Benenson, R.; Franke, U.; Roth, S.; and Schiele, B. 2016. The cityscapes dataset for semantic urban scene understanding. In *CVPR*, 3213–3223.
- Deng, J.; Dong, W.; Socher, R.; Li, L.-J.; Li, K.; and Fei-Fei, L. 2009. ImageNet: A large-scale hierarchical image database. In *CVPR*, 248–255.
- Everingham, M.; Eslami, S. A.; Van Gool, L.; Williams, C. K.; Winn, J.; and Zisserman, A. 2015. The pascal visual object classes challenge: A retrospective. *IJCV*, 111: 98–136.
- Gao, S.; Li, Z.-Y.; Yang, M.-H.; Cheng, M.-M.; Han, J.; and Torr, P. 2022. Large-scale Unsupervised Semantic Segmentation. *IEEE TPAMI*.
- Hamilton, M.; Zhang, Z.; Hariharan, B.; Snavely, N.; and Freeman, W. T. 2022. Unsupervised semantic segmentation by distilling feature correspondences. *ICLR*.
- He, K.; Zhang, X.; Ren, S.; and Sun, J. 2016. Deep residual learning for image recognition. In *CVPR*, 770–778.
- Healthcare Intelligence Laboratory. 2017. SimpleCRF. <https://github.com/HiLab-git/SimpleCRF>.
- Ho, J.; Jain, A.; and Abbeel, P. 2020. Denoising diffusion probabilistic models. *NeurIPS*, 33: 6840–6851.
- Hoffman, J.; Tzeng, E.; Park, T.; Zhu, J.-Y.; Isola, P.; Saenko, K.; Efros, A.; and Darrell, T. 2018. CyCADA: Cycle-consistent adversarial domain adaptation. In *ICML*, 1989–1998. Pmlr.
- Hu, E. J.; Shen, Y.; Wallis, P.; Allen-Zhu, Z.; Li, Y.; Wang, S.; Wang, L.; and Chen, W. 2022. LoRA: Low-rank adaptation of large language models. *ICLR*.
- Hugging Face. 2023a. DreamBooth fine-tuning with LoRA. https://huggingface.co/docs/peft/task_guides/dreambooth_lora.
- Hugging Face. 2023b. Stable-Diffusion-v1-4. <https://huggingface.co/CompVis/stable-diffusion-v1-4>.
- Jo, S.; and Yu, I.-J. 2021. Puzzle-CAM: Improved localization via matching partial and full features. In *ICIP*, 639–643. IEEE.
- Kataoka, H.; Hayamizu, R.; Yamada, R.; Nakashima, K.; Takashima, S.; Zhang, X.; Martinez-Noriega, E. J.; Inoue, N.; and Yokota, R. 2022. Replacing labeled real-image datasets with auto-generated contours. In *CVPR*, 21232–21241.
- Krähenbühl, P.; and Koltun, V. 2011. Efficient inference in fully connected CRFs with gaussian edge potentials. *NeurIPS*, 24.
- Li, D.; Ling, H.; Kim, S. W.; Kreis, K.; Fidler, S.; and Torralba, A. 2022a. BigDatasetGAN: Synthesizing ImageNet with pixel-wise annotations. In *CVPR*, 21330–21340.
- Li, Y.; Duan, Y.; Kuang, Z.; Chen, Y.; Zhang, W.; and Li, X. 2022b. Uncertainty estimation via response scaling for pseudo-mask noise mitigation in weakly-supervised semantic segmentation. In *AAAI*, volume 36, 1447–1455.
- Li, Y.; Kuang, Z.; Liu, L.; Chen, Y.; and Zhang, W. 2021. Pseudo-mask matters in weakly-supervised semantic segmentation. In *ICCV*, 6964–6973.
- Li, Z.; Zhou, Q.; Zhang, X.; Zhang, Y.; Wang, Y.; and Xie, W. 2023. Guiding Text-to-Image Diffusion Model Towards Grounded Generation. *arXiv preprint arXiv:2301.05221*.
- Liu, S.; Liu, K.; Zhu, W.; Shen, Y.; and Fernandez-Granda, C. 2022. Adaptive early-learning correction for segmentation from noisy annotations. In *CVPR*, 2606–2616.
- MMSegmentation Contributors. 2020. MMSegmentation: OpenMMLab Semantic Segmentation Toolbox and Benchmark. <https://github.com/open-mmlab/mms Segmentation>.
- Mokady, R.; Hertz, A.; Aberman, K.; Pritch, Y.; and Cohen-Or, D. 2022. Null-text Inversion for Editing Real Images using Guided Diffusion Models. *arXiv preprint arXiv:2211.09794*.
- Oquab, M.; Bottou, L.; Laptev, I.; and Sivic, J. 2015. Is object localization for free?-weakly-supervised learning with convolutional neural networks. In *CVPR*, 685–694.
- Otsu, N. 1979. A threshold selection method from gray-level histograms. *IEEE transactions on systems, man, and cybernetics*, 9(1): 62–66.
- Radford, A.; Kim, J. W.; Hallacy, C.; Ramesh, A.; Goh, G.; Agarwal, S.; Sastry, G.; Askell, A.; Mishkin, P.; Clark, J.; et al. 2021. Learning transferable visual models from natural language supervision. In *ICML*, 8748–8763. PMLR.
- Ramesh, A.; Pavlov, M.; Goh, G.; Gray, S.; Voss, C.; Radford, A.; Chen, M.; and Sutskever, I. 2021. Zero-shot text-to-image generation. In *ICML*, 8821–8831. PMLR.
- Rao, Y.; Zhao, W.; Chen, G.; Tang, Y.; Zhu, Z.; Huang, G.; Zhou, J.; and Lu, J. 2022. DenseCLIP: Language-guided dense prediction with context-aware prompting. In *CVPR*, 18082–18091.

Richter, S. R.; Vineet, V.; Roth, S.; and Koltun, V. 2016. Playing for data: Ground truth from computer games. In *ECCV*, 102–118. Springer.

Rombach, R.; Blattmann, A.; Lorenz, D.; Esser, P.; and Ommer, B. 2022. High-resolution image synthesis with latent diffusion models. In *CVPR*, 10684–10695.

Rong, S.; Tu, B.; Wang, Z.; and Li, J. 2023. Boundary-Enhanced Co-Training for Weakly Supervised Semantic Segmentation. In *CVPR*, 19574–19584.

Ruiz, N.; Li, Y.; Jampani, V.; Pritch, Y.; Rubinstein, M.; and Aberman, K. 2023. DreamBooth: Fine tuning text-to-image diffusion models for subject-driven generation. In *Proceedings of the IEEE/CVF Conference on Computer Vision and Pattern Recognition*, 22500–22510.

Sariyildiz, M. B.; Alahari, K.; Larlus, D.; and Kalantidis, Y. 2023. Fake it till you make it: Learning transferable representations from synthetic ImageNet clones. In *CVPR*.

Schuhmann, C.; Vencu, R.; Beaumont, R.; Kaczmarczyk, R.; Mullis, C.; Katta, A.; Coombes, T.; Jitsev, J.; and Komatsuzaki, A. 2021. Laion-400m: Open dataset of clip-filtered 400 million image-text pairs. *NeurIPS workshop*.

Shin, G.; Xie, W.; and Albanie, S. 2022. ReCo: Retrieve and co-segment for zero-shot transfer. *NeurIPS*, 35: 33754–33767.

Tian, Y.; Fan, L.; Isola, P.; Chang, H.; and Krishnan, D. 2023. StableRep: Synthetic Images from Text-to-Image Models Make Strong Visual Representation Learners. *arXiv preprint arXiv:2306.00984*.

Wang, Y.; Zhang, J.; Kan, M.; Shan, S.; and Chen, X. 2020. Self-supervised equivariant attention mechanism for weakly supervised semantic segmentation. In *CVPR*, 12275–12284.

Wu, W.; Zhao, Y.; Shou, M. Z.; Zhou, H.; and Shen, C. 2023. Diffumask: Synthesizing images with pixel-level annotations for semantic segmentation using diffusion models. *arXiv preprint arXiv:2303.11681*.

Xu, J.; Liu, S.; Vahdat, A.; Byeon, W.; Wang, X.; and De Mello, S. 2023. Open-vocabulary panoptic segmentation with text-to-image diffusion models. In *CVPR*, 2955–2966.

Yu, P.; Xie, S.; Ma, X.; Zhu, Y.; Wu, Y. N.; and Zhu, S.-C. 2021. Unsupervised foreground extraction via deep region competition. *NeurIPS*, 34: 14264–14279.

Zhou, B.; Khosla, A.; Lapedriza, A.; Oliva, A.; and Torralba, A. 2016. Learning deep features for discriminative localization. In *CVPR*, 2921–2929.

Zhou, C.; Loy, C. C.; and Dai, B. 2022. Extract Free Dense Labels from CLIP. In *ECCV*.